Unusual effects of ammonium ligno-sulphonate on the electrochemical behaviour of lead, lead–calcium, and lead–antimony alloys

A. Tabe Mohammadi, V. S. Donepudi, M. Girgis and W. A. Adams
Electrochemical Science and Technology Centre, University of Ottawa, Ottawa, Ont. KIN LNS (Canada)

(Received October 31, 1991; in revised form July 8, 1992)

Abstract

Ammonium ligno-sulphonate (ALS), is used as a negative plate additive in lead/acid batteries. This compound exerts beneficial effects on lead/acid battery performance by producing a porous film that enhances the reactant and product transport. However, from electrochemical studies conducted in this laboratory, it is shown that the beneficial effects of ALS are restricted to conditions when prior hydrogen evolution did not take place during charging.

Introduction

Certain chemical additives, known as 'expanders' in the lead/acid battery industry, are usually added to lead alloy anodes in order to improve the operational characteristics of lead/acid batteries. These additives adsorb onto the negative plates during discharge and open the pore structure of the lead sulphate films, thereby sustain the transport processes across the battery electrode/electrolyte interface over extended periods of time. One conventional expander formulation often used in lead/acid batteries is a mixture of ammonium ligno-sulphonate (ALS), barium sulphate and carbon black.

The ALS is a sulfonated derivative of lignin, a natural product of wood, and has a complex structure with phenyl propane units with C=O, CHO, and –OH functional groups.

The effects of ligno-sulphonate salts were studied by Mahato [1–3], Pavlov [4], Simon [5], and Brennan and Hampson [6–8]. The studies by Mahato [1–3] included the effects of cations, e.g., Ca^{2+}, Na^{+}, and NH_4^{+}, of ligno-sulphonate compounds. Using the cyclic voltammetry technique, Mahato reported that the anodic dissolution current at the anodic peak potential varied parabolically as a function of ligno-sulphonate concentration, i.e., an increase in current up to 10 ppm of ALS followed by a decrease at higher concentrations. His voltammetry studies were conducted within the potential interval that did not include hydrogen evolution.

In the present study, opposite effects of ALS were observed when the cathodic end potential limit was extended into the hydrogen evolution region [9, 10]. These are new observations not reported before. Therefore, in this paper, these new results, together with some explanations for the observed behaviour, are presented. Cyclic voltammetry and potentiostatic transient techniques supplemented by scanning electron microscopy (SEM) were used in these studies.

0378-7753/92/$5.00

Experimental

The nominal compositions of lead, lead–calcium, and lead–antimony alloys were: 99.99 wt.% Pb, Pb/0.09 wt.% Ca, and Pb/1.66 wt.% Sb, respectively. These alloys were provided by Cominco Metals–Product Technology Centre, Mississauga, Ont., Canada.

The electrodes, 0.8 cm × 0.8 cm in size (apparent geometric area = 0.64 cm^2) were mounted in hard plastic. They were polished on 200, 400 and 600 grit SiC papers, rinsed thoroughly with distilled water, and then were briefly (3 s) etched in 50% nitric acid solution to remove the strained, polishing debris layer.

The electrochemical studies were performed in a single compartment glass cell. Unstirred 30% sulphuric acid solutions at room temperature, 23 ± 1 °C, were used. Saturated calomel electrode (SCE, E = 0.240 V_H) and lead electrode were used as reference and counter electrode respectively for cyclic voltammetry experiments. The measured potentials are reported with respect to the SCE scale through this paper. The effect of ALS was studied under the following conditions: (i) ALS concentrations: 0, 10, 30 and 50 ppm, and (ii) scan rates: 10, 30, 50, 70, 100, 150 and 200 mV s^{-1}.

The cyclic voltammograms were obtained within the potential interval from −1300 mV to −350 mV by commencing the sweep at −1300 mV.

The potentiostatic transients were obtained by prepolarizing the electrode for 15 s at −1300 mV, a potential negative to the hydrogen evolution potential, and then by stepping the potential to the anodic peak potentials that were observed during the cyclic voltammetry experiments. The current at −1300 mV were approximately 200 mA. The reason for prepolarization is to reduce prior passive film.

Results and discussion

Effect of ammonium ligno-sulphonate on electrochemical parameters

Rest potentials

The effects of concentration of ALS on the rest potential of lead, lead–calcium, and lead–antimony alloys are shown in Fig. 1. The rest potentials were shifted to less negative values, i.e., in the cathodic direction as the ALS concentration was increased from 10 ppm to 50 ppm.

Cyclic voltammetry curves

Several cyclic voltammetry curves were obtained for lead, lead–calcium, and lead–antimony alloys under conditions stated in the experimental section. A typical cyclic voltammogram of a lead electrode obtained at a scan rate of 50 mV s^{-1} in stirred H_2SO_4 with 10 ppm ALS added, is shown by solid line in Fig. 2. In this curve, an anodic peak potential corresponding to the maximum dissolution rate, a cathodic peak potential corresponding to reduction of lead sulphate film followed by an inflection corresponding to the onset of the hydrogen evolution reaction can be observed. In the same Figure, another voltammogram similar to those obtained by Mahato [3] is shown as a dashed line. The peak potentials are identical, but the magnitude of current is higher for the dashed line. An increase in the peak anodic current as observed in Mahato's work (similar to the dashed line here) is due to cycling not being done in hydrogen evolution potential range.

From the cyclic voltammetry curves, the peak anodic potential (PAP), peak anodic current density (PAC), and hydrogen evolution potential (HEP) were estimated after five cycles. This information was useful to assess and interpret the effects of ALS on

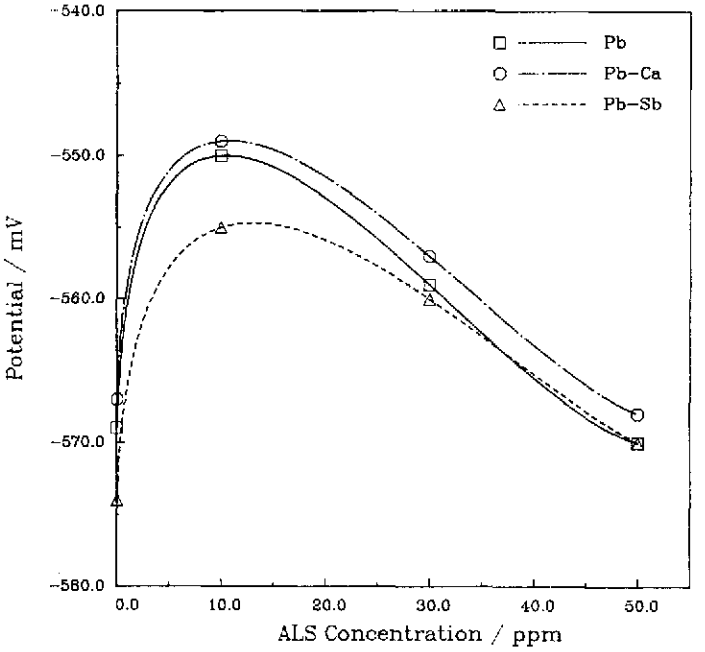

Fig. 1. Effect of ALS concentration on the rest potential of lead and lead alloy anodes in 30% unstirred sulphuric acid solutions at 23±1 °C.

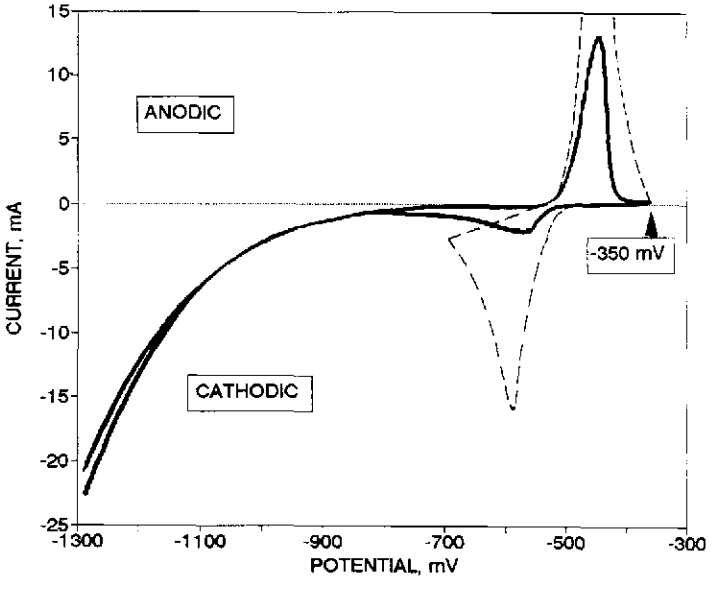

Fig. 2. Typical cyclic voltammograms of lead electrodes in 30% unstirred sulphuric acid solution cycled at the sweep rate of 50 mV/s. Potential intervals: solid line, –1300 mV to –350 mV; dashed line, –700 mV to –350 mV.

lead or lead alloy electrode behaviour in the sulphuric acid solutions. The effects of the concentration of ALS on PAP, PAC, HEP, and Tafel slopes are shown in Figs. 3 to 6. In addition the role of diffusion control is illustrated in Fig. 7, a plot of log scan rate versus log peak anodic current density.

The effect of ALS concentration on the PAP is shown in Fig. 3. The effect is the same as that on the rest corrosion potential, i.e., an increase in the rest potential (anodic shift) with concentration up to 10 ppm followed by a decrease (cathodic shift) at higher concentrations of ALS up to 50 ppm.

The PACs, decreased with an increase in the ALS concentrations, reached a minimum at 10 ppm and then changed slightly at higher concentration up to 50 ppm. A decrease in current density with an increase in ALS concentration is a symptom of passivation in the presence of ALS. Also, in presence of ALS, lead–calcium alloy is likely to passivate easier than lead–antimony or lead.

The effect of ALS concentration on the HEP is shown in Fig. 5. The HEP was shifted in the cathodic direction with an increase in the ALS concentration. This means that in practice lead/acid batteries containing ALS may be changed at slightly higher voltages without hydrogen evolution. The optimum ALS concentration for maximum polarization of the hydrogen evolution reaction is still 10 ppm.

There is a discrepancy between the results of the present studies and those reported previously [1–8]. An important favourable effect of ligno-sulphonate salts, i.e., an increase in the peak anodic current density with an increase in the peak potential was not observed in these studies, e.g., the results in Fig. 4 could be considered as an approximate mirror image of Mahato's results (normal operation of electrode,

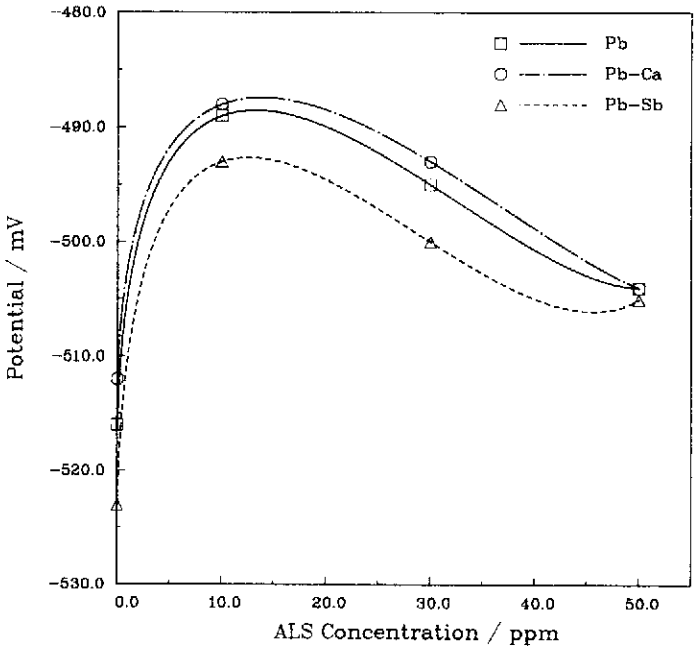

Fig. 3. Peak anodic potential of lead and lead alloy anodes at different ALS concentrations. Experimental conditions: 30% sulphuric acid solution at 23±1 °C , sweep rate: 50 mV/s.

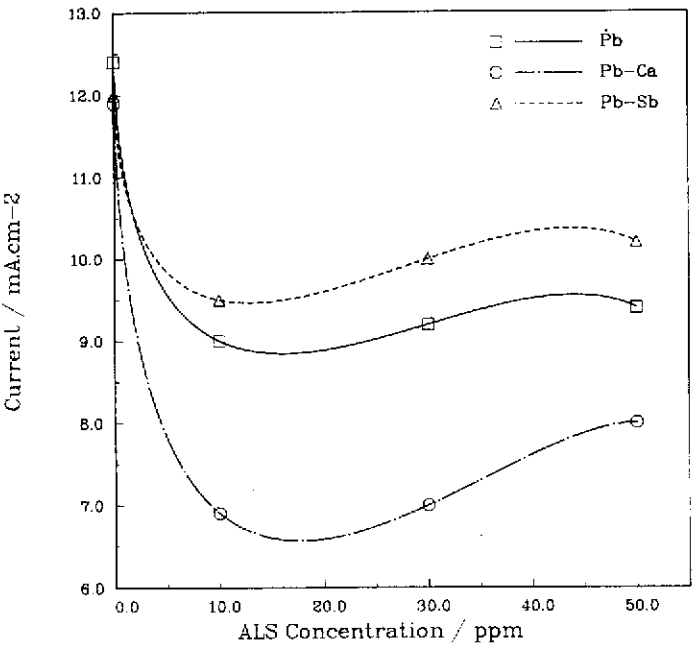

Fig. 4. Peak anodic current density of lead and lead alloy anodes at different ALS concentrations. Experimental conditions as in Fig. 3.

no hydrogen evolution) [2]. The reason for observing the opposite behaviour of ALS to what was observed in other studies is due to the difference in the potential interval within which the cyclic voltammetry studies were performed. All previously reported cyclic voltammetry studies [3] were performed within a potential interval of approximately –800 mV to –350 mV with respect to SCE. An examination of the published voltammograms within the above interval of potentials indicates that hydrogen does not evolve at –800 mV. Some of the cyclic voltammetry experiments that were performed by Mahato [2, 3] within –800 mV to –350 mV potential limits (with respect to SCE) were repeated by us and his results indicative of the beneficial effects of ALS were confirmed (see Fig. 2). In the present studies, hydrogen evolution takes place at the cathodic end potential of –1300 mV.

The present observation related to the ALS effects might be due to: (i) expulsion of trapped ALS within the lead sulphate film by evolving hydrogen, thus allowing larger crystallites to grow, thereby enhancing the passivity, and/or (ii) chemical breakdown of the functional groups of ligno-sulphonate in the presence of hydrogen.

Additional cyclic voltammetry studies were conducted at 10 ppm of ALS and different scan rates in order to establish the status of activation control from the Tafel slopes, and diffusion control from the log peak anodic current density versus log scan rate relationships. The results are shown in Figs. 6 and 7. The Tafel slopes, as calculated from the peak anodic potential versus log scan rate plots shown in Fig. 6 were 30 ± 2 mV. This is a value that is typical for a two electron transfer reaction, i.e., Pb/Pb^{2+}. A slope of 0.5 has been estimated from the straight lines in log scan rate versus log peak anodic current density plots in Fig. 7. The anodic current varies as

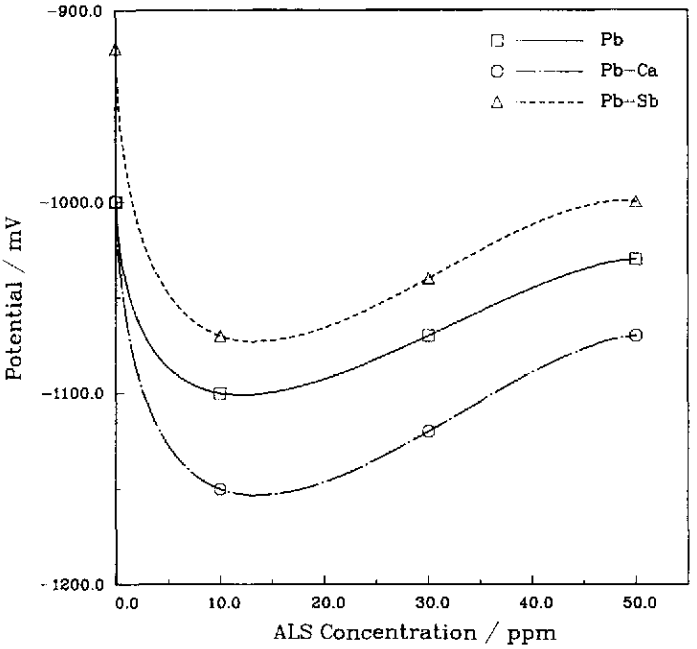

Fig. 5. Hydrogen evolution potential of lead and lead alloy anodes at different ALS concentrations. Experimental conditions as in Fig. 3.

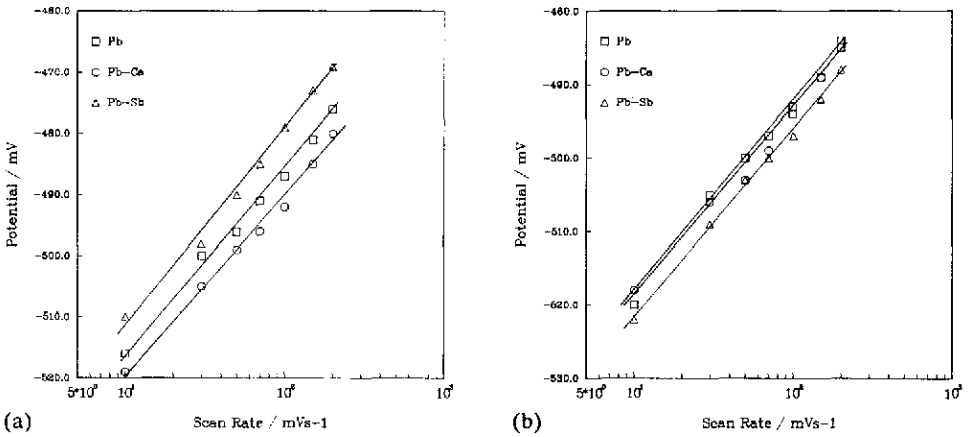

Fig. 6. Tafel plots of lead and lead alloy anodes (a) with no ALS added to the electrolyte, and (b) with 10 ppm ALS added to the electrolyte.

the square root of the scan rate which is indicative of a diffusion controlled process in the vicinity of the peak potential. The process can be related to the passivation of the lead electrode around the anodic peak.

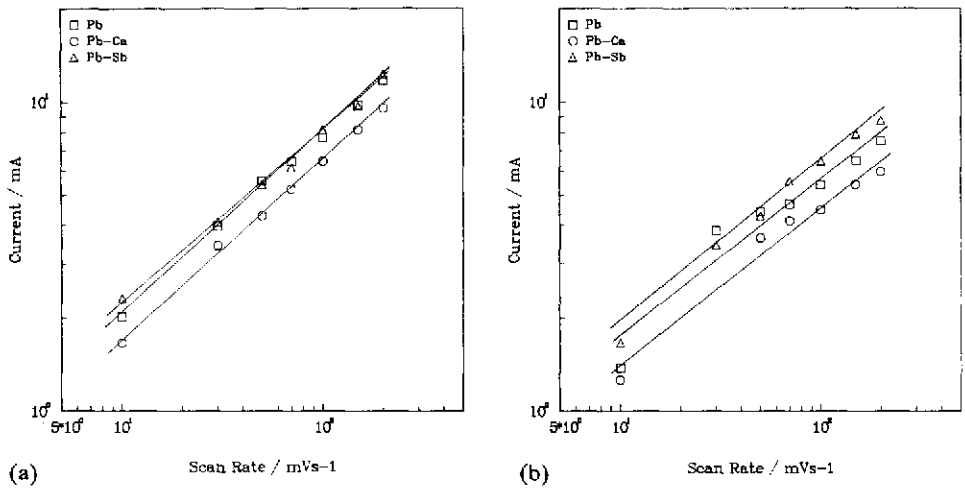

Fig. 7. The variation of the current density with the scan rate (a) with no ALS added to the electrolyte, and (b) with 10 ppm ALS added to the electrolyte.

Potential transients

The potentiostatic transients, i.e., current–time curves at constant potential are shown in Fig. 8. The transients were obtained with and without ALS for lead, lead–calcium, and lead–antimony alloys. These curves have been analysed and mathematically modeled using the transition times estimated from the transients. A dissolution-precipitation model appeared appropriate and an equation describing this model is given below:

$$i = \left(\frac{2nF\pi MN_0k^2ht}{\rho} \right) \exp(-\pi M^2N_0k^2t^2/\rho^2) \tag{1}$$

where n is the number of electron transferred in the electrochemical reaction, F is the Faraday constant (96500 C), M is the molecular weight (g mol^{-1}), N_0 is the number of nuclei formed on unit surface area of electrode, k is rate constant (mol s^{-1} cm^{-2}), h is the height of the nuclei (cm), t is the time (s), and ρ is the density (g cm^{-3}).

Effect of ALS on morphology of lead sulphates

The results from cyclic voltammetry and transient experiments were verified by surface analyses of postpolarized lead alloys using scanning electron microscopy (SEM). The SEM analyses were performed on the electrodes after 5 cycles, and the aged electrodes after 500 cycles. Some specimens were also conditioned in sulphuric acid containing ALS.

The SEM morphologies of lead–calcium anodes before and after different electrochemical treatments are shown in Figs. 9 to 11. Figure 9 shows the surface morphology of a lead–calcium anode before undergoing any electrochemical process. The surface is porous and no deposition has occurred on the surface. The high porosity of the electrode creates a high contact area between the active material and the electrolyte. This effect increases the consumption of the active materials before passivation by lead sulphate, thereby the electrode cycle life. The results of cycling the anode after 5 and 500 cycles in an electrolyte solution with no ALS added, is shown in Fig. 10.

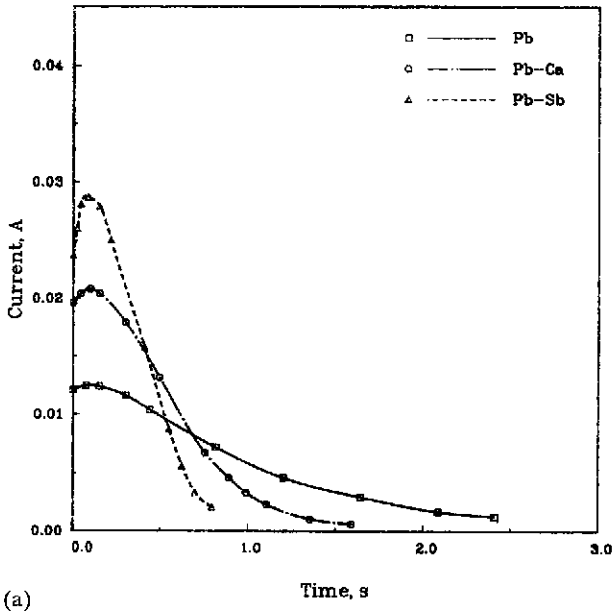

(a)

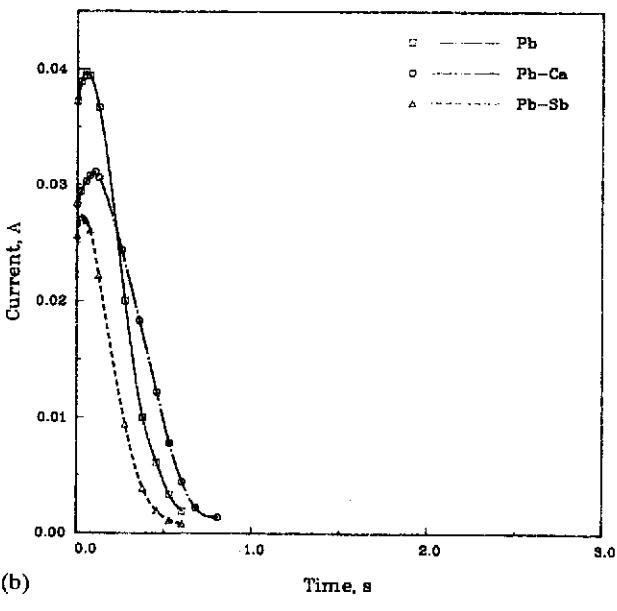

(b)

Fig. 8. Comparison of the transients of lead and lead alloy anodes at their peak anodic potentials (a) with addition of 10 ppm ALS and (b) without addition of ALS to the electrolyte.

After 5 cycles, the surface is covered with fine needle-shaped lead sulphate crystals. The fine crystals cover the surface area, but because of their small size they do not block the pore openings. The growth of dendritic lead sulphate was observed after

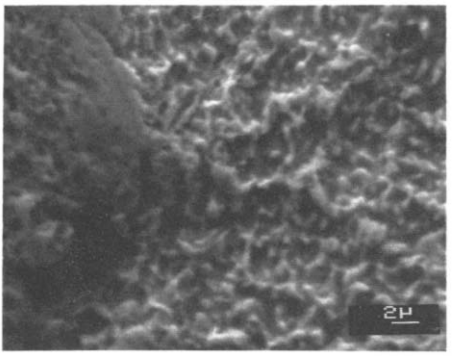

Fig. 9. Scanning electron micrographs of a polished lead–calcium alloy anode before electrochemical treatment.

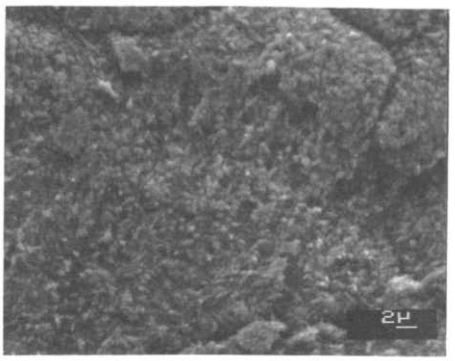

(a)

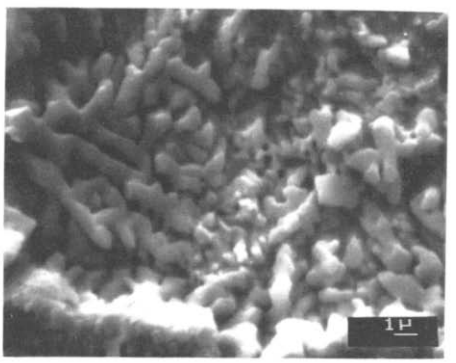

(b)

Fig. 10. Scanning electron micrographs illustrating the deposition of lead sulphate crystals on the surface of a lead calcium alloy anode in absence of ALS (a) after 5 cycles and (b) 500 cycles. Note the formation of dendrites after 500 cycles. Experimental conditions as in Fig. 3.

500 cycles (Fig. 10). The dendrites are fully developed, overlapped, and cover the electrode surface. The formation of large individual lead sulphate crystals was also observed beside the dendritic sites. The formation of both types of lead sulphate are reported in the literature. Identical morphologies were observed for lead and lead–antimony alloys. The size of the crystals was estimated to be in the range of 0.3 to 1.3 μ. The large crystals known as 'hard' lead sulphate, and dendrites block the pore openings and decreases the electrolyte/electrode contact area considerably. It was found that these crystals were not reducible under cathodic charging, in agreement with Pavlov [4]. Therefore, these crystals render the electrode passive during the subsequent discharge cycles, thus shortening the electrode life.

The morphology of lead sulphate crystals in the presence of ALS is shown in Fig. 11. The addition of ALS eliminated the formation of dendrite sites. However, under the combination of hydrogen evolution and ALS addition, the deposits, although not in dendrite shape, tended to be more uniform and adherent compared to Mahato's SEM photographs [1–3], thus enhancing the electrode passivation.

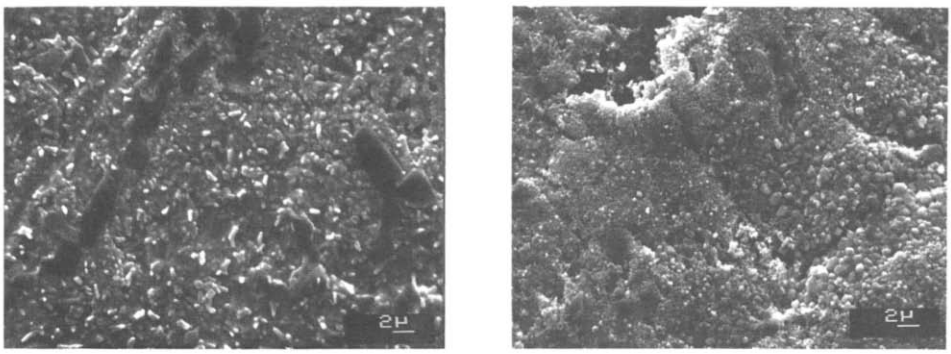

(a) (b)

Fig. 11. Scanning electron micrographs illustrating the formation of lead sulphate crystals on the surface of a lead–calcium alloy anode in the presence of 10 ppm ALS, after (a) 5 cycles and (b) 500 cycles. Note the smaller size of crystals and elimination of dendrites. Experimental conditions as in Fig. 3.

Acknowledgements

The authors would like to express their gratitude to Dr Edward Ghali and Mr Alain Adnot of Laval University, Quebec, Que., Canada, for their generous help in providing surface analysis facilities in that university, and Dr E. Valeriote, Cominco Metal Ltd., Mississauga, Ont., Canada, for supplying the lead alloys. Financial support to this project was provided by the University Research Incentive Fund (URIF) of the province of Ontario, Canada, Westinghouse Canada, and Integrated Power Corporation, MD, USA. A portion of this paper was presented at the 41st Meeting of the International Society of Electrochemistry, August 20–25, 1990, in Prague, Czechoslovakia. The financial support for travel was provided by the University of Ottawa and the City of Nepean, Canada.

References

1 B. K. Mahato, *J. Electrochem. Soc., 124* (1977) 1663–1667.
2 B. K. Mahato, *J. Electrochem. Soc., 127* (1980) 1679–1687.
3 B. K. Mahato, J. Electrochem. Soc., 128 (1981) 1416–1422.
4 D. Pavlov and R. Popova, *Electrochim. Acta, 15* (1970) 1483–1491.
5 A. C. Simon, S. M. Caulder, P. J. Gurlusky and J. R. Pierson, *Electrochim. Acta, 19* (1974) 739–743.
6 M. P. J. Brennan and N. A. Hampson, *J. Electroanal. Chem., 48* (1973) 465–474.
7 M. P. J. Brennan and N. A. Hampson, *J. Electroanal. Chem., 52* (1974) 1–10.
8 M. P. J. Brennan and N. A. Hampson, *J. Electroanal. Chem., 54* (1974) 263–268.
9 A. Tabe Mohammadi, *Electrochemistry of Lead and Alloy Anodes in Lead/Acid Batteries for Photovoltaic Energy Storage, M. A. Sc. Thesis,* University of Ottawa, Ottawa, Ont. Canada, 1990.
10 A. Tabe Mohammadi, V. S. Donepudi, M. Girgis and W. A. Adams, *Effects of Ammonium Ligno-Sulphonate on the Behaviour of Lead and Lead–Calcium Anodes in 30% Sulphuric Acid Solution,* in *Proc. 41st Meet. International Society of Electrochemistry, Prague, Czechoslovakia, Aug. 1990.*